ISSN 0025-6544, Mechanics of Solids, 2021, Vol. 56, No. 6, pp. 911–921. © Allerton Press, Inc., 2021.
Russian Text © The Author(s), 2021, published in Izvestiya Rossiiskoi Akademii Nauk, Mekhanika Tverdogo Tela, 2021, No. 6, pp. 33–44.

Seismic Barriers for Protection Against Surface and Headwaves: Multiple Scatters and Metamaterials

N.F. Morozov[a,b], V.A. Bratov[a,b,c,*], and S.V. Kuznetsov[d,e,f]

[a] *Institute for Problems in Mechanical Engineering, Russian Academy of Sciences, St. Petersburg, 199178 Russia*

[b] *Saint-Petersburg State University, St. Petersburg, 199034 Russia*

[c] *Peter the Great St.Petersburg Polytechnic University, St. Petersburg, 195251 Russia*

[d] *Ishlinskii Institute for Problems in Mechanics, Russian Academy of Sciences, Moscow, 119526 Russia*

[e] *Bauman Moscow State Technical University, Moscow, 105005 Russia*

[f] *Moscow State University of Civil Engineering, Moscow, Russia*

**e-mail: vladimir@bratov.com*

Received March 11, 2021; revised March 18, 2021; accepted March 29, 2021

Abstract—Perspective types of seismic barriers used to protect buildings and structures from the influence of Rayleigh, Rayleigh – Lamb, and Love acoustic surface waves, as well as head SP waves are considered. The barriers are based on multiple scattering elements and metamaterials. A comparison is made with traditional types of homogeneous seismic barriers made of elastic structural materials.

Keywords: seismic waves, seismic barriers, Rayleigh waves, Rayleigh – Lamb waves, Love waves, head SP waves

DOI: 10.3103/S0025654421060133

1. INTRODUCTION

Seismic barriers are designed to protect buildings and structures from seismic surface waves of various etiologies, including Rayleigh waves, Rayleigh – Lamb waves (waves propagating in a layered half-space), Love waves, as well as head SP waves. The latter are a very dangerous type of seismic waves arising from short-focus earthquakes and underground explosions [1–5]. In this article, vertical seismic barriers that contain both special scattering elements and metamaterials with increased dissipation of wave energy are considered.

Below we give an overview of the main types of seismic waves that require vertical seismic barriers to allow protection.

1.1. Rayleigh Waves.

Rayleigh waves are the most common and well-studied type of surface waves arising in a homogeneous elastic half-space. These waves are characterized by (i) frequency-independent propagation speed (no dispersion); (ii) exponential decay of the amplitudes of displacements in depth and localization of wave energy in a relatively narrow surface layer, which allows these waves to propagate over much greater distances, compared to bulk waves [6, 7]; and (iii) the ratio between the displacement components, at which the vertical component of the wave is approximately one and a half times larger than the horizontal one [7]. The latter circumstance makes this type of waves especially dangerous for extended structures. The features associated with the localization of the energy of these waves in the near-surface layer of the earth's crust lead to the fact that Rayleigh waves can bend around the earth several times, see Fig. 1, which shows a seismogram of the arrival of Rayleigh waves that circled the globe eight times [8].

In the recent past, the homogeneous half-space model has been widely used to study wave processes during earthquakes and underground explosions; see [9], where it is noted that Rayleigh waves can also arise during deep-focus earthquakes. In addition, these waves are generated by moving rail and road vehicles [10, 11]. At present, in geophysical and geotechnical applications, the homogeneous half-space model

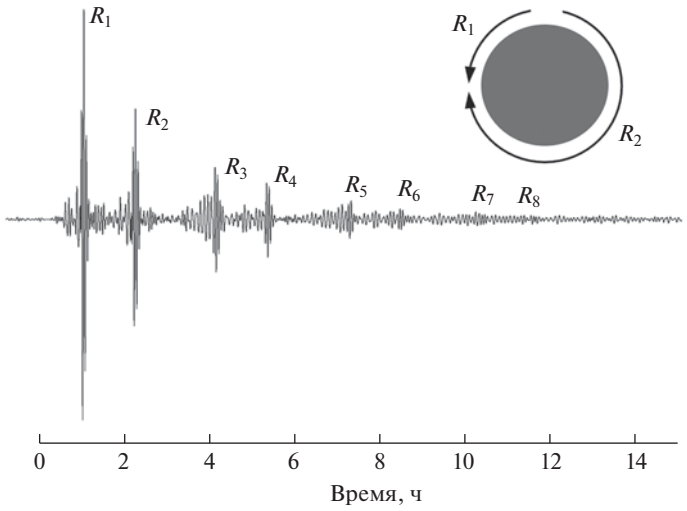

Fig. 1. Seismogram of the Rayleigh wave arrival at the CMB station, Berkeley Digital Seismic Network (BDSN), observation time ~14 h [8]

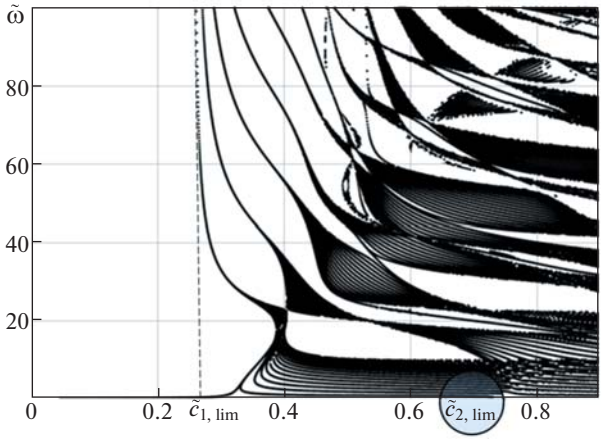

Fig. 2. Dispersion curves for Rayleigh – Lamb waves in a multilayer half-space: horizontal axis – phase velocity; vertical axis – circular frequency

is replaced by the models of layered or functionally gradient half-spaces, in which the propagation of Rayleigh – Lamb dispersive waves is considered [12].

1.2. Rayleigh – Lamb Waves.

The next type of seismic waves is Rayleigh – Lamb waves, which propagate in a layered half-space. A distinctive feature of such waves is dispersion, i.e. the dependence of the speed on frequency, if we consider the Rayleigh – Lamb harmonic waves, Fig. 2.

Despite the very complex dispersion pattern shown in Fig. 2, from the point of view of seismic effects from earthquakes on structures, the so-called second limiting phase velocity, defined as the following limit, is of great interest

$$c_{2,\mathrm{lim}} = \lim_{\omega \to 0} c(\omega) \tag{1.1}$$

where c is the phase velocity and ω is the angular frequency. In layered systems, the velocity $c_{2,\mathrm{lim}}$ is determined either by various low-frequency asymptotic methods [13–15], or by direct calculation using the limiting formula (1.1).

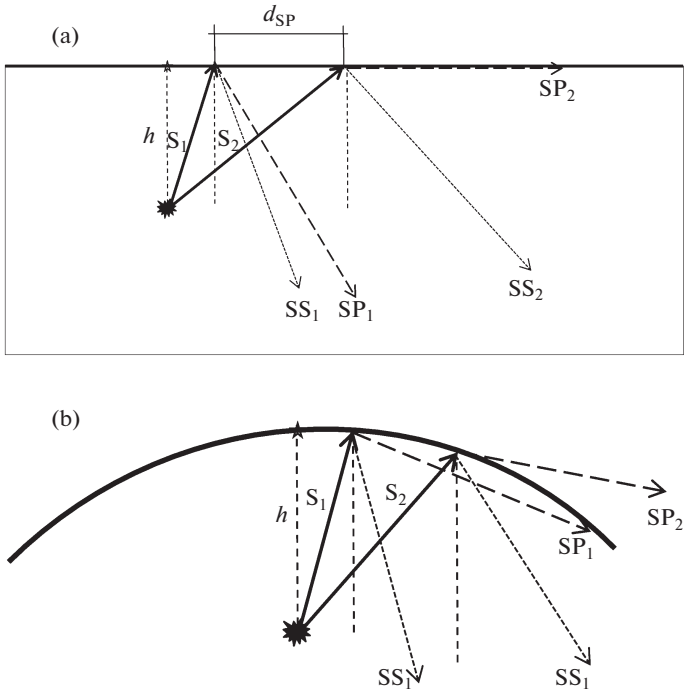

Fig. 3. Schemes of head waves occurrence: a) half-space; b) part of a spherical surface; S1 and S2 are shear waves diverging from the hypocenter of an earthquake or underground explosion, SP2 is (true) head wave; in fig. 2b wave SP1 is quasi head

1.3. Love Waves.

Like the Rayleigh – Lamb waves, Love waves are dispersive waves propagating in an elastic half-space system and an elastic layer (or several layers) in contact with it. Love waves are horizontally transversely polarized and decay exponentially with depth.

From the point of view of seismology, Love waves are mainly of interest in connection with small-amplitude microseisms generated by waves in the ocean [19, 20]. At the same time, during strong earthquakes, the amplitudes of Love waves do not reach the values characteristic of bulk S waves and Rayleigh – Lamb waves [21, 22]. Nevertheless, vertical seismic barriers can also be used to protect against Love waves [23, 24].

1.4. Head SP Waves.

The head SP waves propagate parallel to the free surface of the half-space with the speed of P waves and arise at some distance from the epicenter of a short-focus earthquake or underground explosion, Fig. 3. This distance depends on the source depth h and the physical properties of the medium [25–27], and

$$d_{ST} = h \cdot \tan\left(\arcsin\left(\frac{c_S}{c_P}\right)\right) \tag{1.2}$$

where c_S and c_P are the velocities of transverse and longitudinal body waves, respectively.

In fig. 3 wave S_1 falls on the free surface, forming reflected waves: transversal (SS_1) and longitudinal (SP_1), in a similar way, wave S_2 falls on the free surface, forming reflected waves (SS_2) and longitudinal (SP_2), the latter moves parallel to the free surface by forming a head wave. The angle at which the S_2 wave falls is called the critical angle, it is determined by the following expression [27]:

$$\alpha^* = \arcsin\left(\frac{c_S}{c_P}\right) \tag{1.3}$$

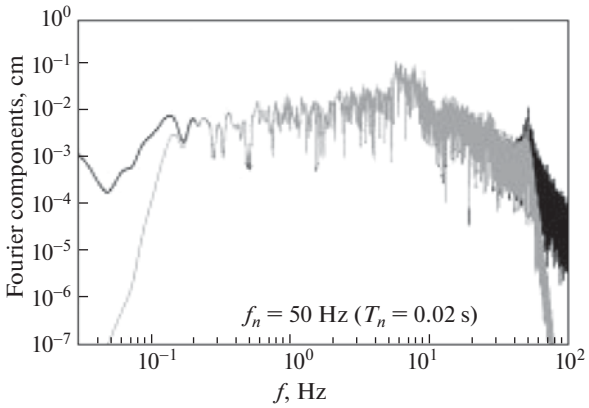

Fig. 4. Fourier amplitude spectrum (FAS), Gebze-Arçelik station, aftershock of the Düzce earthquake (Turkey) 11.11.1999 [29]

Since head or quasi-head waves can carry significant energy and lead to catastrophic destruction [1, 2], vertical seismic barriers, similar to those used to protect against Rayleigh – Lamb waves, are required to protect against these waves.

1.5. Frequency Ranges.

For the design of seismic protection systems against the types of seismic waves under consideration, rough estimates of the frequency range in which a significant proportion of seismic energy is localized are required.

According to estimates [28–31], during natural earthquakes, the most dangerous for most buildings and structures, including nuclear power facilities, are frequencies of 2–33 Hz with energy peaks in the region of 5–7 Hz and 30–33 Hz, Fig. 4.

Artificial earthquakes caused by underground explosions are usually distinguished by higher frequencies [32, 33]. For example, according to [32], frequencies up to 250 Hz are recorded at close distances from the epicenter (limited by the resolution of accelerometers). With increasing distance, high frequencies attenuate and individual bursts are detected at frequencies up to 40 Hz; the maximum amplitudes are recorded at a frequency of ~25 Hz.

1.6. Propagation Velocities of Seismic Waves in the Upper Parts of the Earth's Crust.

To select the geometric and physical parameters of seismic barriers, in addition to the frequency of seismic waves, knowledge of the propagation velocities of bulk and Rayleigh waves is required. According to numerous experimental studies [34–36], the propagation velocities of seismic waves in the upper parts of the earth's crust have the following values, see Table 1.

The propagation velocity of a Rayleigh wave can be determined either as a root of the Rayleigh equation, or by one of the approximate formulas [37, 38], while Poisson's ratio is determined from the corresponding velocities of bulk waves:

$$\nu = \frac{1}{2}\frac{c_P - 2c_S}{c_P - c_S} \tag{1.4}$$

Table 1. Velocities of propagation of bulk waves in the rocks of the earth's crust

Rocks	P wave speed, m/s	S wave speed, m/s
Fluvial	1400	200
Alluvial	1500	250
Moraines	2000	700
Root breeds	4000	2500

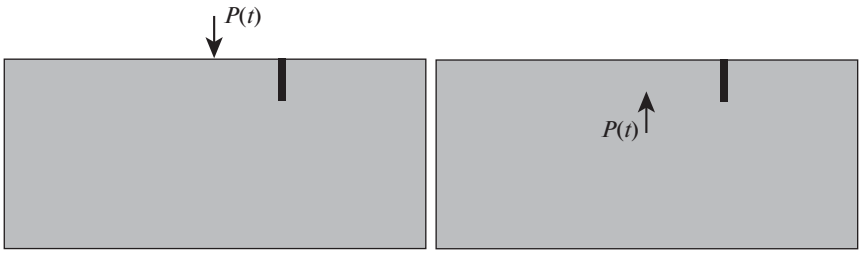

Fig. 5. (a) External and (b) Internal Lamb Problems with Vertical Barriers

1.7. Mathematical Models for the Study of Vertical Barriers.

Usually, for modeling seismic barriers, either plane finite element models are used. They are associated with the numerical solution of the external Lamb problem, in which it is possible to obtain the necessary Rayleigh wave, Fig. 5a, [23, 39, 40]; or consider the solution of a more complex internal Lamb problem, in which, along with the Rayleigh wave, it is possible to simulate the propagation of the head SP wave, see Fig. 5b [27].

Due to the higher requirements for computational resources, spatial models are used much less frequently to solve the Lamb problem with a barrier, see [41]. In the case when it is necessary to take into account the elastic anisotropy of a half-plane or half-space, the methods of boundary integral equations can be used to solve the Lamb problems with the construction of the corresponding fundamental solutions [42–44].

1.8. Equations of State for Describing Dynamic Deformation of Granular Metamaterials.

To describe the behavior of granular metamaterials under the action of dynamic loads, the equations of the bimodular theory of elasticity during deformation in the elastic zone are usually used [45–47]

$$\boldsymbol{\sigma} = \nabla_{\boldsymbol{\varepsilon}}\Psi(I_{\boldsymbol{\varepsilon}}, II_{\boldsymbol{\varepsilon}}, III_{\boldsymbol{\varepsilon}}) \tag{1.5}$$

where $\boldsymbol{\sigma}$ is the stress tensor, $\boldsymbol{\varepsilon}$ is the strain tensor; Ψ is the scalar hyperelastic potential; $I_{\boldsymbol{\varepsilon}}$, $II_{\boldsymbol{\varepsilon}}$, $III_{\boldsymbol{\varepsilon}}$ are the corresponding invariants of the deformation tensor, and the multi-modularity can be taken into account by a potential of the form

$$\Psi(I_\varepsilon, II_\varepsilon^{\sim}) \equiv \alpha I_\varepsilon^2 + \beta II_\varepsilon^{\sim} + \gamma I_\varepsilon\sqrt{II_\varepsilon^{\sim}} \tag{1.6}$$

where α, β, γ are the elastic constants independent of tensor invariants of deformations. Waves in nonlinear media that are described by potentials of the form (1.6) were studied in [47, 48].

In the case when the deviatorial components of the stress tensor reach the plasticity surface, the equations of plastic flow are used, and along with the Mohr – Coulomb and Drucker – Prager models, critical state models are used, for example, the cam-clay model [49–51], see also [52] on metamaterials with the properties of phonon crystals. From the point of view of seismic protection from the surface waves under consideration, metasurfaces are of considerable interest [53].

2. DESIGN MODELS

Disappointingly, for most problems in wave mechanics, there is no possibility of obtaining exact analytical solutions of the equations describing the behavior of the system. Exact analytical solutions are known only for a narrow range of problems with extremely simple geometry (see, for example, [54] for an almost exhaustive list of available solutions). Such solutions, as a rule, are not applicable to the analysis of real problems, but can be used to validate and assess the accuracy of the developed numerical models. In most cases, the problem posed can be solved only numerically using approximate methods for solving the resulting systems of differential equations (see, for example, [55]).

Using the numerical method, we solve the problem of the interaction of an incident dynamic wave in an elastic half-plane with an inclusion representing a vertical seismic barrier (see Fig. 5). We evaluate the effectiveness of one type or another of seismic barriers (Fig. 6b and 6c) by decreasing the amplitudes of displacements and accelerations at points of the surface behind the seismic barrier in comparison with the solution of a similar problem for a half-plane without a seismic barrier (Fig. 6, a).

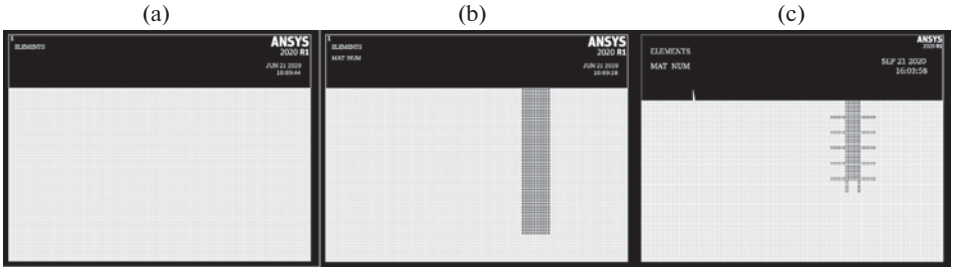

Fig. 6. (a) Elastic half-space without a protective barrier, (b) Elastic half-space with a protective barrier, and (c) Elastic half-space with a barrier with metastructures

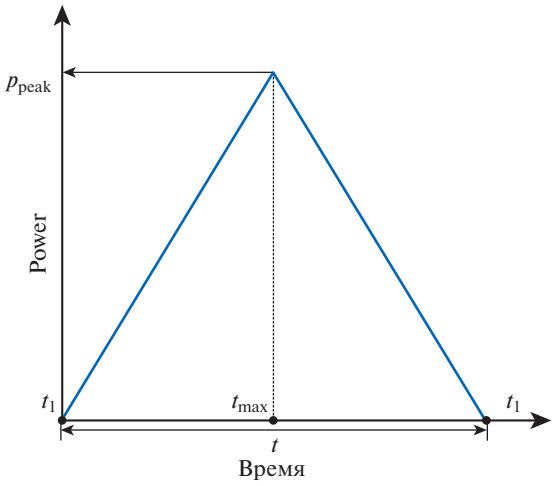

Fig. 7. Time profile of the amplitude of the concentrated force acting on the boundary of the half-plane

Different combinations of elastic properties of the seismic barrier and the metastructures located on the barrier and different geometries of the metastructures are considered.

2.1 Model Problem of the Propagation of an Elastic Wave in an Elastic Half-Plane.

We solve the problem posed numerically using the finite element method. The solutions is obtained using the commercial package ANSYS [57]. At the first stage, we solve the problem of wave propagation in an elastic half-space (Fig. 6a). The wave is excited by a disturbance applied to the surface at a certain distance from the point at which we measure the arising amplitudes of displacements and accelerations. The profile of the dependence of the intensity of the acting force on time is shown in Fig. 7.

On the surface, at some distance from the point of application of the force, we obtain the time dependences of displacements and accelerations along both axes. For this simple problem, the solution can be obtained analytically by calculating the convolution of the solution for the function in time and space and the force applied on the surface (Fig. 7). Such a problem is usually called the two-dimensional exterior Lamb problem, and its analytical solution is known (see, for example, [58]). To validate the obtained numerical solution, let us compare the obtained dependences for displacements with those calculated analytically. Fig. 8 shows the resulting time profile of the displacement for the vertical coordinate, calculated numerically, compared with the analytical exact solution. As can be seen from the presented graphs, the numerical solution reproduces the exact analytical solution quite well. Thus, we can draw a conclusion about the applicability and sufficient accuracy of the obtained numerical solution for solving the studied class of problems.

Further, we obtain the maximum (in time) amplitudes of displacements and accelerations in both directions. Further, these values will be used for normalization when determining the protective coefficient of various types of barriers and protective metastructures. For the used exposure parameters (duration is 450 microseconds, maximum amplitude is 1000 N) and the properties of the medium, taken equal

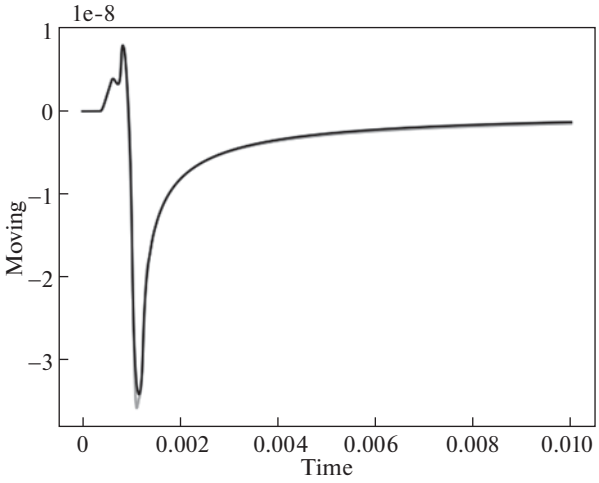

Fig. 8. Temporary displacement profile for the vertical coordinate. Comparison of numerical (gray line) and exact analytical solution (black line)

to those typical for the soil (Young's modulus is E = 10 MPa, Poisson's ratio is Nu = 0.35, density is 2000 kg/m^3), the obtained maximum values of the amplitude of displacements and accelerations in two directions are presented in Table 2.

Next, we use these amplitudes to normalize and determine the protection factor for various types of barriers.

In addition, we investigate the dependence of the maximum amplitude of the arising displacements and accelerations on the distance from the point of application of the load. Such estimates can be carried out both analytically, using an exact solution, and using the developed numerical finite element model. Fig. 9 shows the dependence of the maximum amplitude of the arising horizontal displacements under conditions of the problem being solved.

As can be seen from the data presented in Fig. 9, the numerical solution well repeats the exact analytical solution, which once again indicates the applicability of the developed model for the analysis of the class of problems being solved. In addition, the obtained dependences of the maximum amplitudes of displacements and accelerations will be further used to analyze the so-called "shadow zones" – areas behind protective barriers, in which a significant decrease in displacements and accelerations caused by incident waves of a seismic nature is ensured. The linear size of the "shadow zone" provided by any kind of barrier, along with the protection factor, is one of the most important characteristics of a protective seismic barrier.

Also, based on the analysis of the dependences of the maximum amplitudes of displacements and accelerations on the distance from the point of application of the load, it is possible to estimate the size of the region near the point of application of the load, in which the influence of bulk waves is important.

2.2. More and Less Rigid Barrier.

Further, a similar problem was solved for protective seismic barriers (Fig. 6b) made of two materials, one of which is much more rigid than another one: first material: 1 case – Young's modulus is 10 times greater, the density is 5 times greater; 2 case – Young's modulus is 100 times greater, the density is higher 50 times; second material: 1 case – Young's modulus is 10 times less, the density is 5 times less. 2 case – Young's modulus is 100 times less, the density is 50 times less. For case 1, the typical protection factors of the barriers (the ratio of the maximum displacement/acceleration value in the absence of a barrier to the same value when using a barrier) for the selected case are 1.5–3.0 for accelerations and about the same for displacements. In case 2, the typical protection factors of the barriers for the selected case are 10–25 for accelerations and 1.5–3.0 for movements.

2.3. Metastructure Barriers.

Further, the problem was solved for protective seismic barriers with integrated metastructures (Fig. 6c). Various combinations of elastic properties of barriers and metastructures were considered. In addition, the

Table 2. Velocities of propagation of bulk waves in the rocks of the earth's crust

Maximum acceleration value along the horizontal axis	72.3 m/s^2
The minimum value of the acceleration along the horizontal axis	−43.9 m/s^2
Maximum acceleration value along the vertical axis	110.7 m/s^2
Minimum acceleration value along the vertical axis	−104.7 m/s^2
Maximum displacement value along the horizontal axis	4.70E-07 m
Minimum value of movement along the horizontal axis	−1.40E-07 m
Maximum value of movement along the vertical axis	1.20E-07 m
Minimum value of movement along the vertical axis	−7.50E-07 m

influence of the number and size of the components of metastructures on the provided protection factors was investigated.

As shown by the calculations, in some cases the use of metastructures integrated into the protective seismic barrier can significantly increase the protection factor. In particular, for some cases (for example, a softer (with respect to the medium) barrier with more rigid (with respect to the medium) metastructures), the magnitude reduction factors can reach 30. In other words, with such a configuration of the load and protective barrier, displacement and accelerations in the protected area decrease 30 times. At the same time, some combinations of barrier properties and protective metastructures do not increase the coefficient of protection compared to a barrier without metastructures, or even slightly decrease it. It can be concluded that for specific cases of the properties of the material of the medium, the possible properties and dimensions of the protective barrier and metastructures, it is necessary to carry out additional analysis in order to identify the most effective combinations of the protective barrier for a specific case of possible effects of a seismic nature.

3. CONCLUSION

It has been established by theoretical and numerical studies that, within the framework of the considered elastic models, using vertical seismic barriers in the form of metastructures, it is possible to significantly reduce the magnitude values of oscillations in the protected zone, in comparison with monogenic rectangular barriers, and the level of vibration reduction in the shadow zones behind the barrier turns out to be significantly larger.

In addition, the studies carried out indicate a significant increase in the length of the shadow zone, which opens up prospects for the use of metastructural seismic barriers to protect extended objects, for example, runways of airfields, bridges, aqueducts, etc.

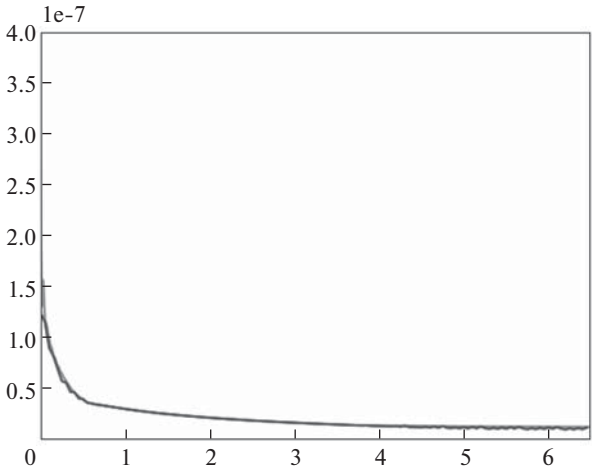

Fig. 9. Dependence of the maximum amplitude of horizontal displacements arising on the surface of the half-plane on the distance from the point of load application. Comparison of numerical (gray line) and exact analytical solution (black line)

FUNDING

This study was supported by the Russian Science Foundation, Grant 20-49-08002.

REFERENCES

1. V. Cerveny, *Seismic Ray Theory* (Cambridge Uni. Press, Cambridge, 2001).
2. P. D. Smith and J. G. Hetherington, *Blast and Ballistic Loading of Structures* (Butterworth-Heinemann, Oxford, 1994).
3. N. Nagy, M. Mohamed, J. C. Boot, "Nonlinear numerical modelling for the effects of surface explosions on buried reinforced concrete structures," Geomech. Eng. **2**, 1–18 (2010). https://doi.org/10.12989/GAE.2010.2.1.001
4. Y. E. Ibrahim and M. Nabil, "Finite element analysis of pile foundations under surface blast loads," in *Proceedings of the 13th International Conference on Damage Assessment of Structures. Lecture Notes in Mechanical Engineering*, Ed. by M. Wahab (Springer, Singapore, 2020).
5. D.V. Helmberger and S. D. Malone, "Modeling local earthquakes as shear dislocations in a layered half-space," J. Geophys. Res. **80**, 4881–4888 (1975).
6. A. Ben-Menahem and S. J. Singh, *Seismic Waves and Sources*, 2nd Ed. (Dover Publications, New York, 2000).
7. K. Aki and P. G. Richards, *Quantitative Seismology*, 2nd Ed. (University Science Books, 2009).
8. K. Aki, "Earthquake mechanism," Tectonophys. **13**, 423–446 (1972).
9. H. Kanamori and D. L. Anderson, "Theoretical basis of some empirical relations in seismology," Bull. Seismol. Soc. Am. 65, 1073–1095 (1975).
10. Y. B. Yang, H. H. Hung, and D. W. Chang, "Train-induced wave propagation in layered soils using finite/infinite element simulation," Soil Dyn. Earthquake Eng. **23** (4), 263–278 (2003).
11. D. Gunn, G. Williams, H. Kessler, and S. Thorpe, "Rayleigh wave propagation assessment for transport corridors," Proc. Inst. Civil Eng. Transp. **168** (6), 487–498 (2015). https://doi.org/10.1680/jtran.14.00036
12. S. V. Kuznetsov, "Abnormal dispersion of flexural Lamb waves in functionally graded plates," Z. Angew. Math. Phys. **70,** 89 (2019). https://doi.org/10.1007/s00033-019-1132-0
13. J. D. Kaplunov and E. V. Nolde, "Long-wave vibrations of a nearly incompressible isotropic plate with fixed faces," Quart. J. Mech. Appl. Math. **55**, 345–356 (2002). https://doi.org/10.1093/qjmam/55.3.345
14. D. D. Zakharov, M. Castaings, and D. Singh, "Numerical and asymptotic approach for evaluating complex wavenumbers of guided modes in viscoelastic plates," J. Acoust. Soc. Am. **130**, 764–771 (2011). https://doi.org/10.1121/1.3605532
15. S. V. Kuznetsov, "Cauchy formalism for Lamb waves in functionally graded plates," J. Vibr. Contr. **25** (6), 1227–1232 (2019). https://doi.org/10.1177/1077546318815376
16. M. Mallah, L. Philippe, and A. Khater, "Numerical computations of elastic wave propagation in anisotropic thin films deposited on substrates," Comp. Mater. Sci. **15**, 411–421 (1999).
17. I. Djeran-Maigre and S. Kuznetsov, "Solitary SH waves in two-layered traction-free plates," Comptes Rendus. Mech. **336** (1–2), 102–107 (2008). https://doi.org/10.1016/j.crme.2007.11.001
18. S. V. Kuznetsov, "Love waves in stratified monoclinic media," Quart. Appl. Math. **62**, 749–766 (2004). https://doi.org/10.1090/qam/2104272
19. T. Saito, "Love-wave excitation due to the interaction between a propagating ocean wave and the sea-bottom topography," Geophys. J. Int. **182**, 1515–1523 (2010). https://doi.org/10.1111/j.1365-246X.2010.04695.x
20. L. Gualtieri, S. J. Camargo, S. Pascale, et al., "The persistent signature of tropical cyclones in ambient seismic noise," Earth Planet Sci. Lett. **484**, 287–294 (2018). https://doi.org/10.1016/j.epsl.2017.12.026
21. A. Ilyashenko and S. Kuznetsov, "SH waves in anisotropic (monoclinic) media," Z. Angew. Math. Phys. **69**, 17 (2018). https://doi.org/10.1007/s00033-018-0916-y
22. G. Ekstrom, J. Tromp, and E. W. F. Larson, "Measurements and global models of surface wave propagation," J. Geophys. Res. 102, 8137–8157 (1997).
23. A. V. Dudchenko, D. Dias, and S. V. Kuznetsov, "Vertical wave barriers for vibration reduction," Arch. Appl. Mech. **91**, 257–276 (2021). https://doi.org/10.1007/s00419-020-01768-2

24. S. Kuznetsov, "Seismic waves and seismic barriers," Acoust. Phys. **57** (3), 420–426 (2011). https://doi.org/10.1134/S1063771011030109
25. E. Kausel and G. Manolis, *Wave Motion in Earthquake Engineering* (WIT Press., Southampton, UK, 1999).
26. O. V. Angelsky, C. Y. Zenkova, S. G. Hanson, and J. Zheng, "Extraordinary manifestation of evanescent wave in biomedical application," Front. Phys. **8**, 159 (2020). https://doi.org/10.3389/fphy.2020.00159
27. S. V. Kuznetsov and E. O. Terentjeva, "Planar internal Lamb problem: Waves in the epicentral zone of a vertical power source," Acoust. Phys. 61, 356–367 (2015). https://doi.org/10.1134/S1063771015030112
28. N. N. Ambraseys, J. Douglas, P. Smit, and S. K. Sarma, "Equations for the estimation of strong ground motions from shallow crustal earthquakes using data from Europe and the Middle East: horizontal peak ground acceleration and spectral acceleration," Bull. Earthquake Eng. **3** (1), 1–53 (2005). https://doi.org/10.1007/s10518-005-0183-0
29. S. Akkar, O. Kale, E. Yenier, and J. J. Bommer, "The high-frequency limit of usable response spectral ordinates from filtered analogue and digital strong-motion accelerograms," Earthquake Eng. Struct. Dyn. **40** (12), 1387–1401 (2011).
30. I. Takewaki, "Frequency-domain analysis of earthquake input energy to structure–pile systems," Eng. Struct. **27** (4), 549–563 (2005). https://doi.org/10.1016/j.engstruct.2004.11.014
31. I. Takewaki, "Response spectrum method for nonlinear surface ground analysis," Int. J. Adv. Struct. Eng. **7** (6), 503–514 (2004). https://doi.org/10.1260/1369433042863233
32. X. Li, Z. Li, E. Wang, et al., "Spectra, energy, and fractal characteristics of blast waves," J. Geophys. Eng. 15 (1), 81–92 (2017). https://doi.org/10.1088/1742-2140/aa83cd
33. M. Bahadori, H. B. Amnieh, and A. Khajezadeh, "A new geometrical-statistical algorithm for predicting two-dimensional distribution of rock fragments caused by blasting," Int. J. Rock Mech. Mining Sci. **86**, 55–64 (2016). https://doi.org/10.1016/j.ijrmms.2016.04.002
34. O. Uyanik, "Estimation of the porosity of clay soils using seismic P- and S-wave velocities," J. Appl. Geophys. **170**, 103832 (2019). https://doi.org/10.1016/j.jappgeo.2019.103832
35. *Recommended Provisions for Seismic Regulations for New Buildings and Other Structures. Part 1. Provisions (FEMA 450-2), 2003 Edition. Building Seismic Safety Council* (National Institute of Building Sciences, Washington, D.C., 2004).
36. *International Handbook of Earthquake and Engineering Seismology*. Part B, Ed. by W. H. K. Lee, Kanamori H. Hiroo, P. C. Jennings, and C. Kisslinger (Academic Press, New York, 2003).
37. Chi Vinh Pham and P. G. Malischewsky, "An approach for obtaining approximate formulas for the Rayleigh wave velocity," Wave Motion. **44** (7–8), 549–562 (2007). https://doi.org/10.1016/j.wavemoti.2007.02.001
38. V. G. Mozhaev, "Approximate analytical expressions for the velocity of Rayleigh waves in isotropic media and on the basal plane in high symmetry crystals," Sov. Phys. Acoust. **37**, 186-189 (1991).
39. V. A. Bratov et al., "Homogeneous horizontal and vertical seismic barriers: mathematical foundations and dimensional analysis," Mat. Phys. Mech. **44** (1), 61–65 (2020). https://doi.org/10.18720/MPM.4412020_7
40. A.V. Kravtsov, S. V. Kuznetsov, and S. Y. Sekerzh-Zen'kovich, "Finite element models in Lamb's problem," Mech. Solids. **46**, 952–959 (2011). https://doi.org/10.3103/S002565441106015X
41. A. Pecker, "Seismic analyses and design of foundation soil structure interaction," in *Perspectives on European Earthquake Engineering and Seismology. Geotechnical, Geological and Earthquake Engineering*, Vol. 39, Ed. by A. Ansal (Cham, Springer, 2015), pp. 153–162. https://doi.org/10.1007/978-3-319-16964-4_6
42. E. Kausel, "Lamb's problem at its simplest," Proc. Roy. Soc. Ser. A. London. **469** (2149), 20120462 (2012). https://doi.org/10.1098/rspa.2012.0462
43. S. V. Kuznetsov, "Fundamental and singular solutions of Lamé equations for media with arbitrary elastic anisotropy," Quart. Appl. Math. **63**, 455–467 (2005). https://doi.org/10.1090/S0033-569X-05-00969-X
44. F. Sánchez-Sesma and U. Iturrarán-Viveros, "The classic Garvin's problem revisited," Bull. Seism. Soc. Am. **96** (4A), 1344–1351 (2006). https://doi.org/10.1785/0120050174

45. V. P. Maslov and P. P. Mosolov, "General theory of the solutions of the equations of motion of an elastic medium of different moduli," J. Appl. Math. Mech. **49** (3), 322–336 (1985). https://doi.org/10.1016/0021-8928(85)90031-0
46. V. P. Maslov and M. M. Antsiferova, "Shock waves in a granular medium," Phys. Earth. Planet. Inter. **50** (1), 8-15 (1988).
47. S. N. Gavrilov and G. C. Herman, "Wave propagation in a semi-infinite heteromodular elastic bar subjected to a harmonic loading," J. Sound Vibr. **331** (20), 4464–4480 (2012). https://doi.org/10.1016/j.jsv.2012.05.022
48. A. Molinari and Ch. Daraio, "Stationary shocks in periodic highly nonlinear granular chains," Phys. Rev. E **80** (5), 056602 (2009). https://doi.org/10.1103/PhysRevE.80.056602
49. R. V. Goldstein, et al., "The modified Cam-Clay (MCC) model: cyclic kinematic deviatoric loading," Arch. Appl. Mech. **86**, 2021-2031 (2016). https://doi.org/10.1007/s00419-016-1169-x
50. S. V. Kuznetsov and H. Maigre, "Granular metamaterials for seismic protection. Hyperelastic and hypoelastic models," J. Phys.: Conf. Ser. **1425** (012184), 1–6 (2019). https://doi.org/10.1088/1742-6596/1425/1/012184
51. R. M. Nedderman, *Statics and Kinematics of Granular Materials* (Cambridge Univ. Press, Cambridge, 2005).
52. W. Witarto, S. J. Wang, C. Y. Yang, et al., "Three-dimensional periodic materials as seismic base isolator for nuclear infrastructure," AIP Adv. **9**, 045014 (2019). https://doi.org/10.1063/1.5088609
53. P. T. Wootton, J. Kaplunov, and D. J. Colquitt, "An asymptotic hyperbolic–elliptic model for flexural-seismic metasurfaces," Proc. R. Soc. A. **475**, 20190079 (2019). https://doi.org/10.1098/rspa.2019.0079
54. E. Kausel, Fundamental Solutions in Elastodynamics (Cambridge Univ. Press, Cambridge, 2005). https://doi.org/10.1017/CBO9780511546112
55. V. Bratov, "Incubation time fracture criterion for FEM simulations," Acta Mech. Sinica **27** (4), 541–549 (2011). https://doi.org/10.1007/s10409-011-0484-2
56. N. Kazarinov, V. Bratov, and Y. Petrov, "Modelling dynamic propagation of a crack at quasistatic loading," Dokl. Phys. **59** (2), 99–102 (2014). https://doi.org/10.1134/S1028335814020116
57. *ANSYS User's Guide, Release 2020 R1* (ANSYS Inc., Pennsylvania, USA, 2020).
58. A. C. Eringen and E. S. Suhubi, *Elastodynamics* Vol. 2: *Linear Theory* (Academic Press, New York, 1975).

Translated by A.A. Borimova

SPELL; OK